TargetM6A: Identifying N^6-methyladenosine Sites from RNA Sequences via Position-Specific Nucleotide Propensities and a Support Vector Machine

Guang-Qing Li, Zi Liu, Hong-Bin Shen, and Dong-Jun Yu*

***Abstract*—As one of the most ubiquitous post-transcriptional modifications of RNA, N^6-methyladenosine (m^6A) plays an essential role in many vital biological processes. The identification of m^6A sites in RNAs is significantly important for both basic biomedical research and practical drug development. In this study, we designed a computational-based method, called TargetM6A, to rapidly and accurately target m^6A sites solely from the primary RNA sequences. Two new features, i.e., position-specific nucleotide / dinucleotide propensities (PSNP / PSDP), are introduced and combined with the traditional nucleotide composition (NC) feature to formulate RNA sequences. The extracted features are further optimized to obtain a much more compact and discriminative feature subset by applying an incremental feature selection (IFS) procedure. Based on the optimized feature subset, we trained TargetM6A on the training dataset with a support vector machine (SVM) as the prediction engine. We compared the proposed TargetM6A method with existing methods for predicting m^6A sites by performing stringent jackknife tests and independent validation tests on benchmark datasets. The experimental results show that the proposed TargetM6A method outperformed the existing methods for predicting m^6A sites and remarkably improved the prediction performances, with *MCC* = 0.526 and *AUC* = 0.818. We also provided a user-friendly web server for TargetM6A, which is publicly accessible for academic use at http://csbio.njust.edu.cn/bioinf/TargetM6A.**

***Index Terms*—N^6-methyladenosine, RNA methylation, position-specific nucleotide propensity, incremental feature selection, support vector machine.**

Manuscript received xx xx, 2016; revised xx xx, 2016; accepted xx xx, 2016. Date of publication xx xx, 2016; date of current version xx xx, 2016. This work was supported by the National Natural Science Foundation of China (No. 61373062 and 61222306), the Natural Science Foundation of Jiangsu (No. BK20141403), the China Postdoctoral Science Foundation (Nos. 2014T70526 and 2013M530260), the Fundamental Research Funds for the Central Universities (No. 30916011327), the Science and Technology Commission of Shanghai Municipality (No. 16JC1404300), and "The Six Top Talents" of Jiangsu Province (No. 2013-XXRJ-022). Asterisk indicates corresponding author.

G.-Q. Li and Z. Liu are with the School of Computer Science and Engineering, Nanjing University of Science and Technology, Xiaolingwei 200, Nanjing, China, 210094.

H.-B. Shen is with the Institute of Image Processing and Pattern Recognition, Shanghai Jiao Tong University, Shanghai 200240, China.

*D.-J. Yu is with the School of Computer Science and Engineering, Nanjing University of Science and Technology, Xiaolingwei 200, Nanjing, China,210094 (e-mail: njyudj@njust.edu.cn).

I. Introduction

POST-translational modification (PTLM) of proteins is an important biological mechanism because it is associated with many major diseases [1]. A similar subtle modification, the so-called post-transcriptional modification (PTCM), may also occur in RNA sequences. The PTCMs of RNA are very common and important in living organisms [2, 3]. To date, more than 100 PTCMs have been discovered in native cellular RNAs, including mRNAs and other RNAs [4, 5]. Among these modifications, N^6-methyladenosine (m^6A) is the most ubiquitous internal modification, which plays an important role in regulating gene expression [6-9]. As shown in Fig. S1 (see Supplementary Material II), methylation occurs on the sixth nitrogen atom of adenine, which is catalyzed by N^6-methyladenosine methyltransferase (a complex composed of METTL3, METTL14, and WTAP) [10, 11], and the reverse process is catalyzed by demethylases (FTO or ALKBH5) [12, 13].

Since it was first identified in mammalian mRNA during the mid-1970s [14], m^6A has been studied for decades to determine its exact functions and mechanisms. A series of studies have proven that m^6A plays an essential role in diverse biological processes. Deng *et al.* discovered that m^6A is important for respiration and stress responses in bacteria [15]; Liu *et al*. found that m^6A can enhance the interaction between RNA and protein by altering the RNA structure [16]; Alarcon *et al*. showed that m^6A can initialize miRNA processing and promote miRNA maturation by marking primary microRNAs (pri-miRNAs) [17]; and several studies have shown that the proteins of the YTH domain family are m^6A-specific RNA-binding proteins that regulate both mRNA stability and localization [8, 18, 19]. All of these scientific findings indicate that knowledge of m^6A is vitally important for both basic biomedical research and practical drug development.

Many studies have been dedicated to identifying the m^6A sites in RNA sequences. Traditional m^6A identification methods, such as thin-layer chromatography (TLC), high-performance liquid chromatography (HPLC), mass spectrometry, and scintillation, heavily depend on physicochemical techniques to study m^6A distribution [20].

Accordingly, these methods are low-throughput and laborious and can only be applied to small-scale datasets [21]. Recently, based on several newly-developed high-throughput m^{6}A profiling techniques (e.g., m^{6}A-seq [21] and MeRIP-Seq [22]), the transcriptome-wide maps of m^{6}A distributions in several species, including *Oryza sativa* [23], *Saccharomyces cerevisiae* [24], *Mus musculus* [25], and *Homo sapiens* [25], have been reported. The results of these studies showed that m^{6}A sites are highly conserved and are not randomly distributed as follows: m^{6}A sites tend to occur near stop codons, 3′ UTRs, and within long internal exons [22, 24, 25]. Although the above-mentioned methods can provide insights into the distributions and characteristics of m^{6}A sites, they are both expensive and time-consuming. With the avalanche of RNA sequences released in the post-genomic era, it is highly desirable to develop computational methods to rapidly and accurately identify m^{6}A sites solely from RNA sequences.

Unfortunately, to the best of our knowledge, there are currently only three computational tools, i.e., iRNAMethyl [26], m6Apred [27], and pRNAm-PC [28], available for predicting m^{6}A sites in RNA sequences. The iRNAMethyl tool identifies m^{6}A sites using an effective pseudo dinucleotide composition (PseDNC) feature, which integrates information about the RNA sequence order with three RNA physicochemical properties [26]. The m6Apred tool exploits nucleotide chemical category feature and accumulated nucleotide frequency feature to encode an RNA sequence [27]. The pRNAm-PC tool derives the RNA sequence feature from the physicochemical properties of the nucleotides via a series of auto-covariance and cross covariance transformations and uses support vector machine as prediction engine [28]. These pioneering studies have shown the feasibility of predicting m^{6}A sites solely from RNA sequences. However, their prediction performances are still relatively low and should be further improved for potential practical applications.

This paper aims to accomplish this task using a novel feature representation method and machine-learning techniques. A new sequence-based m^{6}A site predictor called TargetM6A is developed. In TargetM6A, we first encode each target RNA sequence into a fixed-length feature vector using the newly developed position-specific nucleotide/dinucleotide propensity (PSNP/PSDP) features and the nucleotide composition (NC) feature; then, we obtain an optimized feature subset by applying the incremental feature selection (IFS) algorithm [29-32] to the original feature space. Finally, we train a support vector machine (SVM) [33] prediction model with the optimized feature subset on the training dataset. We compared the proposed TargetM6A method with existing m^{6}A site predictors via stringent jackknife tests and independent validation tests on benchmark datasets, and the results of the comparison show the superiority of the proposed method. Below, we address the detailed procedures for constructing TargetM6A.

II. Materials and Methods

A. Benchmark datasets

Three benchmark datasets, i.e., Met2614 [26], Train1664 [27], and Test5225 [27], were used in this study. All of the three datasets were constructed from 1,183 genes in the *S. cerevisiae* genome. Because the m^{6}A sites in the *S. cerevisiae* genome share a GAC consensus motif that has the potential to be methylated at the center base [24], we can formulate each RNA sample (segment), denoted as $R_\xi(\mathbb{GAC})$, in these datasets as follows:

$$R_\xi(\mathbb{GAC}) = N_{-\xi}N_{-(\xi-1)}\cdots N_{-1}\mathbb{GAC}N_1\cdots N_{+(\xi-1)}N_{\xi} \quad (1)$$

where $N_{-\xi}$ represents the ξ-th upstream nucleotide from the central motif GAC and $N_{+\xi}$ represents the ξ-th downstream nucleotide.

Chen *et al*. [26] constructed Met2614 based on the experimentally determined m^{6}A modification data from the *S. cerevisiae* genome [24]. The positive subset of Met2614 contains 1,307 methylation RNA segments, each of which has an N^6-methylated adenosine at the center position; the negative subset is composed of 1,307 non-methylation RNA segments, each of which also has an adenosine at the center position that is not N^6-methylated. Please note that the value of ξ is 24 and thus the RNA segment length is $2 \times 24 + 3 = 51$ for Met2614. For more details about the procedure used to construct the Met2614 dataset, refer to [26].

Based on Met2614, Chen *et al*. [27] further constructed Train1664 and Test5225 as described below. Among the 1,307 methylation RNA segments in Met2614, 832 segments, whose m^{6}A sites were less than 10 nt from the detected m^{6}A-seq peaks, were selected as the positive Train1664 samples. Then, 832 samples were randomly selected from the 33,280 non-methylated RNA segments and used as the negative Train1664 samples [27]; the remaining 475 (1,307 – 832 = 475) methylation RNA segments in Met2614 and the 4,750 randomly selected samples from the 33,280 non-methylation RNA segments constitute the independent validation dataset, i.e., Test5225. The value of ξ is 9 and thus the RNA segment length is $2 \times 9 + 3 = 21$ for both Train1664 and Test5225. For more details, refer to [27]. All three benchmark datasets used in this study are included in Supplementary Material I or can be freely downloaded from the web server http://csbio.njust.edu.cn/bioinf/TargetM6A.

Please note that in this work we first evaluated a prediction model for Met2614 compared to the jackknife test; then, we evaluated a prediction model for Train1664 compared to the jackknife test and an independent validation test (on Test5225). The final prediction model on the webserver, TargetM6A, is trained on Met2614.

B. Feature representation of the RNA segments

One of the key problems in designing a machine-learning based m^{6}A site predictor is determining how to encode an RNA sample (segment) into a fixed-length feature vector with highly discriminative information. Since the nucleotide composition (NC) feature [34-36] and pseudo nucleotide composition (PseNC) feature [26, 37, 38] were proposed, they have been

This article has been accepted for publication in a future issue of this journal, but has not been fully edited. Content may change prior to final publication. Citation information: DOI 10.1109/TNB.2016.2599115, IEEE Transactions on NanoBioscience

widely utilized for nucleotide sequence representations. However, the performances of these two features for predicting m^{6}A sites are still very low (see the "Results and Discussion" section). Therefore, in this study, two new features, i.e., position-specific nucleotide / dinucleotide propensity (PSNP / PSDP) features, were proposed to encode the RNA segments. Then, the two features were combined with the traditional NC feature to form the discriminative feature vector for predicting the m^{6}A sites.

1) Position-specific nucleotide propensity (PSNP) feature

Position-specific nucleotide / amino acid preferences are widely used in bioinformatics to predict functional sites in biological sequences [39-43]. The principle of position-specific preferences is to compute the frequency at which nucleotides / amino acids occur at certain positions and extract statistical information from sequences. Inspired by previous studies, we introduced a new position-specific nucleotide propensity (PSNP) feature in this study. Next, we describe how to encode an RNA segment into a PSNP feature vector.

Because the RNA segment expressed by (1) contains the consensus motif GAC at its center, we deleted the central GAC of the segment, and the remaining RNA segment can be reformulated as follows:

$$\mathrm{R}_{\xi} = \mathrm{N}_1\mathrm{N}_2\cdots\mathrm{N}_{2\xi} \tag{2}$$

where N_j (j = 1, 2, …, 2ξ) represents the nucleotide at the j-th position of the remaining RNA segment, and can be any one of the 4 nucleotide bases in RNA, i.e., $\mathrm{N}_j \in$ {A (adenine), C (cytosine), G (guanine), U (uracil)}. We term R_{ξ} as a reduced RNA segment.

We first calculated the 4-dimensional position-specific occurrence frequency vector for the 4 nucleotides from the positive reduced RNA segments.

$$\mathbf{z}_j^{+} = [\, z_{1,j}^{+} \quad z_{2,j}^{+} \quad z_{3,j}^{+} \quad z_{4,j}^{+} \,]^T \tag{3}$$

where $z_{i,j}^{+}$ is the occurrence frequency of the nucleotide base type i (i =1, 2, 3, 4) at the j-th (j = 1, 2, …, 2ξ) position. Note that in this case, we use the numerical codes 1, 2, 3, and 4 to represent A (adenine), C (cytosine), G (guanine), and U (uracil), respectively.

Similarly, we can calculate the corresponding 4-dimensional position-specific occurrence frequency vector for the 4 nucleotides from the negative reduced RNA segments.

$$\mathbf{z}_j^{-} = [\, z_{1,j}^{-} \quad z_{2,j}^{-} \quad z_{3,j}^{-} \quad z_{4,j}^{-} \,]^T \tag{4}$$

where $z_{i,j}^{-}$ is the occurrence frequency of the nucleotide base type i (i =1, 2, 3, 4) at the j-th (j = 1, 2, …, 2ξ) position.

We defined the *position-specific frequency difference vector*, denoted as $\mathbf{z}_j$, as follows:

$$\mathbf{z}_j = \mathbf{z}_j^{+} - \mathbf{z}_j^{-} = [\, z_{1,j} \quad z_{2,j} \quad z_{3,j} \quad z_{4,j} \,]^T \tag{5}$$

where $z_{i,j} = z_{i,j}^{+} - z_{i,j}^{-}$, i =1, 2, 3, 4, and j = 1, 2, …, 2ξ.

Based on the position-specific frequency difference vectors, we can obtain a 4 × 2ξ position-specific nucleotide propensity (PSNP) matrix as follows:

$$\mathbf{Z}_{\mathrm{PSNP}} = \begin{bmatrix} \mathbf{z}_1 & \mathbf{z}_2 & \cdots & \mathbf{z}_{2\xi} \end{bmatrix} = \begin{bmatrix} z_{1,1} & z_{1,2} & \cdots & z_{1,2\xi} \\ z_{2,1} & z_{2,2} & \cdots & z_{2,2\xi} \\ z_{3,1} & z_{3,2} & \cdots & z_{3,2\xi} \\ z_{4,1} & z_{4,2} & \cdots & z_{4,2\xi} \end{bmatrix} \tag{6}$$

Now, an RNA segment can be encoded into a 2ξ-dimensional PSNP feature vector, denoted as $\mathbf{f}_{\mathrm{PSNP}}$, by referring to the $\mathbf{Z}_{\mathrm{PSNP}}$:

$$\mathbf{f}_{\mathrm{PSNP}} = [\, f_1 \quad f_2 \quad \cdots \quad f_j \quad \cdots \quad f_{2\xi} \,]^T \tag{7}$$

where each element f_j is selected from the $\mathbf{Z}_{\mathrm{PSNP}}$ matrix according to (8) and defined as follows:

$$f_j = \begin{cases} z_{1,j} \text{ , when } \mathrm{N}_j = \mathrm{A} \\ z_{2,j} \text{ , when } \mathrm{N}_j = \mathrm{C} \\ z_{3,j} \text{ , when } \mathrm{N}_j = \mathrm{G} \\ z_{4,j} \text{ , when } \mathrm{N}_j = \mathrm{U} \end{cases}, \quad (j = 1,2,\cdots,2\xi). \tag{8}$$

2) Position-specific dinucleotide propensity (PSDP) feature

We further extended the PSNP to dinucleotides (double nucleotide) to extract additional information contained in RNA segment. We termed this feature as the position-specific dinucleotide propensity (PSDP) feature. The RNA segment described in (2) could be rewritten in a dinucleotide form:

$$\mathrm{R}_{\xi} = \mathrm{N}_1\mathrm{N}_2\cdots\mathrm{N}_{2\xi} = \mathrm{D}_1\mathrm{D}_2\cdots\mathrm{D}_{2\xi-1} \tag{9}$$

where D_j = $\mathrm{N}_j\mathrm{N}_{j+1}$ (j = 1, 2, …, 2ξ–1) represents the dinucleotide at the j-th position, and can be any of the 16 types of dinucleotides, i.e., $\mathrm{D}_j \in$ {AA, AC, AG, ⋯ ,UU}.

Based on the same principle used to generate the $\mathbf{Z}_{\mathrm{PSNP}}$ matrix, we can calculate the 16 × (2ξ–1) position-specific dinucleotide propensity (PSDP) matrix on a given dataset as follows:

$$\mathbf{Z}_{\mathrm{PSDP}} = \begin{bmatrix} z_{1,1} & z_{1,2} & \cdots & z_{1,2\xi-1} \\ z_{2,1} & z_{2,2} & \cdots & z_{2,2\xi-1} \\ \vdots & \vdots & \ddots & \vdots \\ z_{16,1} & z_{16,2} & \cdots & z_{16,2\xi-1} \end{bmatrix} \tag{10}$$

where $z_{i,j} = z_{i,j}^{+} - z_{i,j}^{-}$, and $z_{i,j}^{+}$ is the occurrence frequency of the dinucleotide type i ($i = 1,2,\cdots,16$) at the j-th (j = 1, 2, …, 2ξ–1) position calculated from the positive reduced RNA segments, whereas $z_{i,j}^{-}$ is the corresponding occurrence frequency derived from the negative reduced RNA segments.

Using $\mathbf{Z}_{\mathrm{PSDP}}$, we can encode each RNA segment into a (2ξ–1)-dimensional PSDP feature vector, denoted as $\mathbf{f}_{\mathrm{PSDP}}$, as follows:

$$\mathbf{f}_{\mathrm{PSDP}} = [\, f_1 \quad f_2 \quad \cdots \quad f_j \quad \cdots \quad f_{2\xi-1} \,]^T \tag{11}$$

where each element is obtained from the $\mathbf{Z}_{\mathrm{PSDP}}$ matrix in (12), which is defined as follows:

$$f_j = \begin{cases} z_{1,j} \text{ , when } \mathrm{D}_j = \mathrm{AA} \\ z_{2,j} \text{ , when } \mathrm{D}_j = \mathrm{AC} \\ \vdots \\ z_{16,j} \text{ , when } \mathrm{D}_j = \mathrm{UU} \end{cases} \quad (j = 1,2,\cdots,2\xi-1). \tag{12}$$

3) Nucleotide composition (NC) feature

Nucleotide composition (NC), i.e., the k-mer nucleotide frequency, is a classic method for representing the features of a

This article has been accepted for publication in a future issue of this journal, but has not been fully edited. Content may change prior to final publication. Citation information: DOI 10.1109/TNB.2016.2599115, IEEE Transactions on NanoBioscience

nucleotide sequence, and has been widely used in previous studies [34-36]. For a given k value, a 4^k-dimensional feature vector is obtained, indicating the frequency of occurrence for each k-mer nucleotide in a nucleotide sequence. In this study, we used k = 1, 2, and 3, i.e., 4 types of *one*-mer nucleotide frequencies, 16 types of *two*-mer frequencies, and 64 types of *three*-mer frequencies. Thus, an 84-dimensional (4 + 16 + 64 = 84) NC feature vector was generated for an RNA segment.

Finally, by serially combining the above-mentioned PSNP, PSDP, and NC features, an M-dimensional feature vector was obtained to represent each RNA segment, where $M = 2\xi + (2\xi - 1) + 84$. Because the value of ξ for Met2614 is 24, the dimensionality of the combined feature vector is 179; however, the dimensionality of the combined feature vector for Train1664 and Test5225 is 119 because the corresponding value of ξ is 9.

C. Incremental feature selection

The aforementioned feature representation procedure encodes each RNA segment into a fixed-length feature vector. We performed an incremental feature selection (IFS) procedure [29-32] based on the statistical F-test [44, 45] to identify the most prominent components of the original feature vector that are beneficial for distinguishing methylated RNA segments from non-methylated segments, as described below.

First, the statistical F-test [44, 45] was employed to measure the significance of all the extracted feature components. More specifically, by performing the F-test, we can obtain the p-value of each feature component according to the feature vectors for both the positive and negative samples in a dataset. A feature component with a smaller p-value was deemed as a more significant feature. Consequently, all the initial feature components were re-ranked by their p-values in ascending order. The set of the re-ranked feature components can be formulated as follows:

$$\left\{ f_1^{'}, f_2^{'}, \cdots, f_M^{'} \right\} \tag{13}$$

where the p-value of $f_i^{'}$ is less than that of $f_j^{'}$ if $i < j$, and M is the dimensionality of the original feature vector, i.e., $M = 2\xi + (2\xi - 1) + 84$.

Second, the incremental feature selection (IFS) [29-32] method was employed to determine the feature components that should be selected for inclusion in the optimal feature subset based on the set of ranked feature components described in (13). After this step, we obtained the M feature subsets as follows:

$$\mathbf{f}_i = \left\{ f_1^{'}, \cdots, f_{i-1}^{'}, f_i^{'} \right\} \quad (i = 1, 2, \cdots, M) \tag{14}$$

where the i-th feature subset is composed of the top i ranked feature components defined in (13).

Finally, we evaluate the discriminative capability of each feature subset over the K-fold (K = 10 in this study) cross-validation using a specific prediction engine, and the subset that achieves the highest *MCC* value will be considered the optimal feature subset. In this study, the support vector machine (SVM) was used as the prediction engine and will be briefly introduced in the next section.

D. SVM as prediction engine

The support vector machine (SVM), which was proposed by Cortes and Vapnik, is a machine-learning algorithm based on the statistical learning theory [33, 46]. It solves nonlinear separable problems by kernel methods, whose basic principle is to transform the input vector into a high-dimensional Hilbert space using kernel functions and to identify the maximal separating hyperplane between classes [46, 47]. This technique has been widely used in a variety of bioinformatics areas [34, 48, 49] and has been shown to be a powerful prediction engine. In this study, we also applied SVM as the prediction engine for constructing the proposed TargetM6A method. The package LIBSVM V3.20 (http://www.csie.ntu.edu.tw/~cjlin/libsvm)

TABLE I
PREDICTION RESULTS OF DIFFERENT FEATURES USING DIFFERENT PREDICTION ENGINES ON THE MET2614 DATASET OVER A 10-FOLD CROSS-VALIDATION [1]

Feature [2]	Prediction engine	*Sen* (%)	*Spe* (%)	*Acc* (%)	*MCC*	*AUC*
PSNP	RF	70.07 (±0.71)	75.29 (±1.13)	72.68 (±0.71)	0.454 (±0.014)	0.777 (±0.006)
	KNN	74.17 (±0.26)	73.22 (±0.46)	73.70 (±0.32)	0.473 (±0.006)	0.783 (±0.001)
	SVM	74.15 (±0.16)	74.43 (±0.12)	74.29 (±0.07)	0.485 (±0.001)	0.790 (±0.001)
PSDP	RF	70.78 (±0.25)	75.40 (±0.24)	73.09 (±0.15)	0.462 (±0.003)	0.784 (±0.001)
	KNN	72.69 (±0.36)	73.56 (±0.31)	73.12 (±0.24)	0.462 (±0.004)	0.779 (±0.001)
	SVM	72.38 (±0.25)	74.85 (±0.36)	73.62 (±0.25)	0.472 (±0.005)	0.788 (±0.001)
NC	RF	61.02 (±0.57)	62.19 (±0.93)	61.60 (±0.43)	0.232 (±0.008)	0.666 (±0.005)
	KNN	69.08 (±0.58)	54.48 (±0.55)	61.78 (±0.51)	0.238 (±0.010)	0.664 (±0.002)
	SVM	64.55 (±0.43)	63.34 (±0.60)	64.45 (±0.38)	0.288 (±0.007)	0.702 (±0.002)
PSNP+PSDP	RF	70.71 (±0.70)	75.88 (±0.44)	73.29 (±0.33)	0.466 (±0.006)	0.784 (±0.002)
	KNN	74.74 (±0.38)	72.78 (±0.19)	73.76 (±0.22)	0.475 (±0.004)	0.785 (±0.001)
	SVM	73.65 (±0.25)	75.39 (±0.24)	74.52 (±0.15)	0.490 (±0.003)	0.792 (±0.001)
PSNP+PSDP+NC	RF	71.80 (±0.80)	76.60 (±0.62)	74.20 (±0.54)	0.484 (±0.010)	0.799 (±0.003)
	KNN	**75.65** (±0.26)	72.54 (±0.30)	74.10 (±0.17)	0.482 (±0.003)	0.793 (±0.001)
	SVM	74.38 (±0.28)	**77.16** (±0.48)	**75.77** (±0.27)	**0.515** (±0.005)	**0.815** (±0.001)

[1] The experiment was performed 10 times for each feature and prediction engine. The average performance of each evaluation index is reported, followed by a standard deviation.

[2] PSNP, PSDP, and NC stand for position-specific nucleotide propensity, position-specific dinucleotide propensity, and nucleotide composition, respectively.

This article has been accepted for publication in a future issue of this journal, but has not been fully edited. Content may change prior to final publication. Citation information: DOI 10.1109/TNB.2016.2599115, IEEE Transactions on NanoBioscience

provided by Chang and Lin [47] was used to implement SVM. The radial basis function (RBF) kernel was chosen. The two parameters contained in the RBF kernel, i.e., the regularization parameter C and the kernel width parameter γ, were optimized based on a 10-fold cross-validation using a grid search strategy. The optimized values of C and γ are both 2 for Met2614 and Train1664.

E. Evaluation indexes

In statistical learning fields, the following three validation methods are often used to evaluate the performance of a predictor: independent dataset test, subsampling (or K-fold cross-validation) test, and jackknife test [50]. In the jackknife test, all the samples in the benchmark dataset will be singled out one-by-one and tested by the predictor trained on the remaining samples [51]. Therefore, the jackknife test is considered the least arbitrary validation method that can always yield a unique outcome for a given benchmark dataset [51]. However, the complexity of the jackknife test is equal to the amount of data in the dataset, making it time-consuming to implement. Therefore, in this study, the 10-fold cross-validation test was utilized to optimize the SVM parameters and select the features, whereas the jackknife test was used to evaluate the performances of the different learning algorithms and provide an unbiased assessment of the performance of the different prediction models.

In literature, Accuracy (*Acc*), Sensitivity (*Sen*), Specificity (*Spe*), and the Matthews correlation coefficient (*MCC*) are routinely used as evaluation indexes [52, 53], which are defined as follows:

$$\begin{cases} Sen = 1 - \dfrac{N_-^+}{N^+} \\ Spe = 1 - \dfrac{N_+^-}{N^-} \\ Acc = 1 - \dfrac{N_-^+ + N_+^-}{N^+ + N^-} \\ MCC = \dfrac{1 - \dfrac{N_-^+ + N_+^-}{N^+ + N^-}}{\sqrt{(1 + \dfrac{N_+^- - N_-^+}{N^+})(1 + \dfrac{N_-^+ - N_+^-}{N^-})}} \end{cases} \quad (15)$$

where N^+ is the total number of the positive samples or true m^{6}A sites, N_-^+ is the number of true m^{6}A sites that were incorrectly predicted to be a non-m^{6}A site, N^- is the total number of the negative samples or non-m^{6}A sites, and N_+^- is the number of non-m^{6}A sites that were incorrectly predicted to be an m^{6}A site. Please note that this set of indexes is only valid for the single-label systems. For the multi-label systems whose existence has become more frequent in system biology [54] and system medicine [55], a completely different set of indexes as defined in [56] is needed.

For a soft-type classifier (e.g., the SVM used in this study), whose outputs are the continuous numerical values representing the probabilities/confidences of a feature belonging to certain classes, gradual adjustments to the discrimination threshold will produce a series of prediction confusion matrices [57]. Each of these confusion matrices generates different corresponding values of N_+^- and N_-^+. In other words, the evaluation indexes defined in (15) are threshold-dependent. Therefore, we also employed another threshold-independent evaluation index, i.e., Area under Curve (*AUC*), which is based on the Receiver Operating Characteristic (ROC) analysis [58]. The *AUC* values range from 0 to 1. The larger the *AUC* value, the better the predictor performs. Specifically, an *AUC* = 0.5 means that the predictor generates a random prediction, whereas an *AUC* = 1 represents a perfect predictor, which always generates the correct prediction.

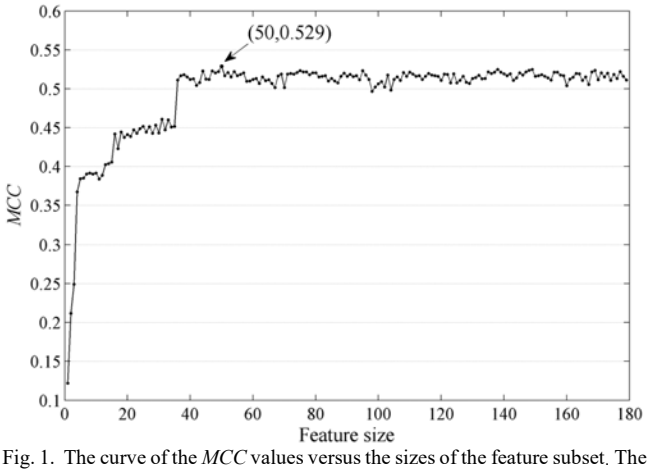

Fig. 1. The curve of the *MCC* values versus the sizes of the feature subset. The maximum *MCC* value is 0.529 and the corresponding feature size is 50.

III. Results and Discussion

A. Contributions of different features

A series of comparative experiments were performed using individual features (i.e., PSNP, PSDP, and NC) and their combinations (i.e., PSNP+PSDP and PSNP+PSDP+NC) to evaluate the contributions of different features to the m^{6}A site predictions. We evaluated the discriminative performances of each of the five features (i.e., three individual features and the two combined features) using three popular prediction engines, i.e., Support Vector Machine (SVM) [33], Random Forests (RF) [59], and K Nearest Neighbor (KNN) [60], over a 10-fold cross-validation. Table 1 summarizes the prediction performances of each feature using the different prediction engines. Note that for each feature and prediction engine, the 10-fold cross-validation experiment was performed 10 times. The average performance of each evaluation index is reported, followed by a standard deviation.

As shown in Table 1, several conclusions can be drawn.

First, for all five types of features, SVM consistently performed better than RF and KNN concerning the two overall evaluation indexes (i.e., *MCC* and *AUC*). This phenomenon indicates that SVM is the most appropriate engine among the three considered engines for predicting m^{6}A sites using the features developed in this study.

Second, for all three prediction engines, the two newly developed features, i.e., PSNP and PSDP, performed

This article has been accepted for publication in a future issue of this journal, but has not been fully edited. Content may change prior to final publication. Citation information: DOI 10.1109/TNB.2016.2599115, IEEE Transactions on NanoBioscience

TABLE II
PREDICTION PERFORMANCES OF THE TOP50 AND ALL179 FEATURE SUBSETS OF THE MET2614 DATASET OVER BOTH THE 10-FOLD CROSS-VALIDATION AND JACKKNIFE TESTS.

Feature subset	10-fold cross-validation			jackknife test		
	Acc (%)	*MCC*	*AUC*	*Acc* (%)	*MCC*	*AUC*
Top50	**76.18** (±0.28)	**0.523** (±0.005)	**0.819** (±0.001)	**76.32**	**0.526**	**0.818**
All179	75.77 (±0.27)	0.515 (±0.005)	0.815 (±0.001)	75.67	0.513	0.816

significantly better than NC. Using the SVM prediction engine as an example, the NC feature achieved a prediction performance with an $MCC < 0.30$ and $AUC < 0.71$, whereas the proposed PSNP and PSDP features achieved much better performance with an $MCC > 0.47$ and $AUC > 0.78$.

Third, the combination of individual features can further improve prediction performance. By revisiting Table I, we found that the combined PSNP+PSDP feature consistently outperformed the individual features, i.e., PSNP and PSDP, for all three prediction engines. On the other hand, the NC feature performed significantly worse than the other two individual features. As illustrated in Table I, the NC feature only achieved an *MCC* of 0.288 and an *AUC* of 0.702 using SVM as the prediction engine. However, we found that the prediction performance can be greatly improved by adding the NC feature to the PSNP+PSDP feature. As shown in Table I, the PSNP+PSDP+NC feature (SVM as prediction engine) achieved the best performance with an *MCC* of 0.515 and an *AUC* of 0.815, which were 2.5% and 2.3%, respectively, better than the PSNP+PSDP feature.

Based on the three observations described above, we used PSNP+PSDP+NC as the input feature and SVM as the prediction engine to construct the proposed TargetM6A method.

B. Feature selection performance

In this section, we will try to further improve the computational efficiency and prediction performance by removing the redundant components in the PSNP+PSDP+NC feature with the incremental feature selection (IFS) procedure described in the "Incremental feature selection" section.

We first obtained the *p*-value for each component of the PSNP+PSDP+NC feature by performing *F*-test [44, 45]. Then, all the initial feature components were re-ranked by their *p*-values in ascending order. The list of the detailed re-ranked feature components for the Met2614 dataset is shown in Table S1 (see Supplementary Material II). Then, based on the ranked feature components, the IFS procedure was applied, and 179 feature subsets (for Met2614) were obtained. We evaluated the discriminative capability (measured by *MCC*) of each feature subset using the SVM prediction engine over a 10-fold cross-validation. Fig. 1 plots the curve of *MCC* values versus the sizes of the feature subset.

As illustrated in Fig. 1, the *MCC* value almost consistently increases when the feature size varies from 1 to 50. The *MCC* value reaches a peak (0.529) when the feature size is 50. When the feature size is larger than 50, the *MCC* value fluctuates and no improvement was observed.

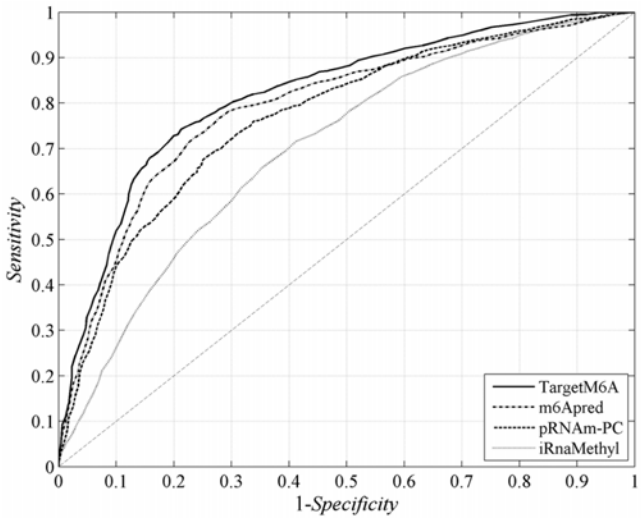

Fig. 2. The ROC curves of iRNAMethyl, m6Apred, pRNAm-PC, and the proposed TargetM6A method. The *AUC* values of these methods are 0.701, 0.762, 0.792, and 0.818, respectively.

To extensively investigate the effectiveness of the feature selection procedure, we further performed the stringent jackknife test (i.e., leave-one-out cross-validation) on the Met2614 dataset with SVM as prediction engine using the following two feature subsets: (1) the optimal feature subset, which consists of the top 50 feature components (denoted as Top50), and (2) the entire feature set, which consists of 179 initial feature components (denoted as All179). Table II summarizes the prediction performances of the two feature subsets on the Met2614 dataset over both the 10-fold cross-validation and jackknife tests.

As shown in Table II, the Top50 feature subset consistently outperformed the All179 feature subset with regard to the three overall evaluation indexes, i.e., *Acc*, *MCC*, and *AUC*, over both the 10-fold cross-validation and jackknife tests. Using the jackknife test as an example, the Top50 feature subset achieved an *Acc* of 76.32%, an *MCC* of 0.526, and an *AUC of* 0.818, which were 0.6%, 1.3%, and 0.2%, respectively, better than those of the All179 feature subset. Similar observations can also be obtained using 10-fold cross-validation. These findings indicate that there is redundant information in the original 179 components, and the 50 selected feature components are truly the "significant" components for identifying the m^6A sites. On one hand, the prediction performance can be slightly improved using the dimensionality-reduced feature subset, i.e., Top50; on the other hand, the computational efficiency is enhanced.

C. Comparisons with existing predictors

In this section, we will compare the proposed TargetM6A method with existing computational methods for predicting m^6A sites, including iRNAMethyl [26], pRNAm-PC [28], and m6Apred [27], to demonstrate its efficacy.

We first compared these m^6A site predictors using the Met2614 dataset and rigorous jackknife tests. The BLAST-based predictor [26] was used as the baseline predictor. The BLAST-based method predicts m^6A sites by applying the sequence similarity search tool, i.e., BLAST [61], as follows: a

This article has been accepted for publication in a future issue of this journal, but has not been fully edited. Content may change prior to final publication. Citation information: DOI 10.1109/TNB.2016.2599115, IEEE Transactions on NanoBioscience

TABLE III
COMPARISON OF THE RESULTS FROM THE PROPOSED TARGETM6A METHOD AND THE EXISTING PREDICTORS ON MET2614 USING JACKKNIFE TESTS.

Prediction methods	*Sen* (%)	*Spe* (%)	*Acc* (%)	*MCC*	*AUC*
BLAST [1]	71.56	38.79	55.27	0.109	-
iRNAMethyl [1]	60.63	70.55	65.59	0.313	0.701
pRNAm-PC [2]	69.72	69.75	69.74	0.394	0.762
m6Apred [3]	73.91	74.45	74.18	0.483	0.792
TargetM6A	**74.83**	**77.81**	**76.32**	**0.526**	**0.818**

[1]Results excerpted from [26].
[2]Results excerpted from [28].
[3]The re-implementation of m6Apred [27] on Met2614.

query sample will be predicted as the true N^6-methylation RNA segment if it is the most similar to the samples in the positive subset; otherwise, it will be predicted as a non-methylated RNA segment [26]. Because m6Apred [27] does not provide results on Met2614, we thus re-implemented it and evaluated it using Met2614. Please note that TargetM6A utilized the reduced feature subset, i.e., Top50, as the feature representation and SVM as the prediction engine. In addition, the default threshold, i.e., 0.5, was used for TargetM6A and the re-implemented m6Apred to produce the *Sen*, *Spe*, *Acc*, and *MCC* values. Table III summarizes the results of the comparison of the different predictors on the Met2614 dataset using the jackknife test, and Fig. 2 compares their ROC curves.

As shown in Table III, we can find that the proposed TargetM6A method significantly outperformed the baseline predictor; the *MCC* value was remarkably improved from 0.109 to 0.526. TargetM6A also outperformed iRNAMethyl [26], pRNAm-PC [28], and m6Apred [27] with respect to all of the five evaluation indexes. Using *MCC* as an example, 21.3%, 13.2%, and 4.3% improvements were observed compared with iRNAMethyl [26], pRNAm-PC [28], and m6Apred [27].

In addition, the ROC curves plotted in Fig. 2, together with the *AUC* values listed in Table III, indicate that TargetM6A achieved the best performance regarding *AUC*. TargetM6A outperformed iRNAMethyl, pRNAm-PC, and m6Apred for the *AUC*, with improvements of 11.7%, 5.6%, and 2.6%, respectively. Considering that the jackknife test is the most rigorous cross-validation method, these experimental results indeed show the superiority of the proposed TargetM6A method over the existing m^6A site predictors.

We further evaluated the efficacy of the proposed method using two other benchmark datasets, i.e., Train1664 and Test5225. Please note that the original feature vector extracted from the Train1664 dataset is 119-D (18-D PSNP, 17-D PSDP, and 84-D NC features), as described in the "Feature representation of RNA segments" section. Then, the IFS procedure was performed and an optimized feature subset of 65 feature components (see Table S2 in Supplementary Material II for details) was obtained to construct the SVM-based prediction model.

We first evaluated TargetM6A on Train1664 using the jackknife test. Then, we trained TargetM6A on Train1664 and tested the trained model with the independent validation dataset, i.e., Test5225. Because only m6Apred [27] currently provides results on Train1664 and Test5225, we only compared the proposed TargetM6A method with m6Apred. The performances of m6Apred were excerpted from a previous study [27]. Table IV summarizes the comparison of the results from m6Apred and the proposed TargetM6A method using the Train1664 and Test5225 datasets.

As shown in Table IV, the proposed TargetM6A method achieved very comparable performances with m6Apred for both Train1644 and Test5225. It has not escaped our notice that TargetM6A achieved much better performance than m6Apred for Met2614 (refer to Table III). However, TargetM6A failed to improve the prediction performance and only achieved comparable performance with m6Apred for Train1644 and Test5225 (refer to Table IV). We speculate that the differences in the RNA segment length and amount of data between Met2614 and Train1644 may account for this phenomenon: the RNA segment length ($\xi = 24$) and data volume (2,614 samples) of Met2614 are much larger than those of the Train1664 dataset ($\xi = 9$, 1,664 samples). Because the proposed method extracts the features according to the distribution of nucleotides in the central GAG motif, a dataset with larger RNA segment length and data volume will contain much more information about the distribution of nucleotides and thus will be beneficial for extracting more discriminative features. We believe that the prediction performance of TargetM6A can be further improved by increasing the number of available methylated and non-methylated RNA samples.

D. Web server implementation

A web server has been placed online at http://csbio.njust.edu.cn/bioinf/TargetM6A to enhance the applicability of the proposed TargetM6A method. The final online TargetM6A method was trained on Met2614, where each training sample is a 51-nt RNA segment. The TargetM6A method predicts m^6A sites as described below.

For a query RNA sequence submitted by a user, TargetM6A first identifies all the GAC motifs in the query sequence; then, for each GAC motif, a corresponding 51-nt RNA segment is constructed by placing a sliding window centered on the GAC motif. Based on the constructed 51-nt RNA segment, the features are extracted and then fed to the SVM classification engine to perform the prediction. Please note that to construct the corresponding 51-nt segment for a GAC motif with an insufficient number of nucleotides around the sequence (e.g., a

TABLE IV
PREDICTION RESULTS OF DIFFERENT FEATURES USING DIFFERENT PREDICTION ENGINES ON THE MET2614 DATASET OVER A 10-FOLD CROSS-VALIDATION [*]

Methods	Train1664					Test5225				
	Sen (%)	*Spe* (%)	*Acc* (%)	*MCC*	*AUC*	*Sen* (%)	*Spe* (%)	*Acc* (%)	*MCC*	*AUC*
m6Apred [*]	79.21	77.04	78.12	0.563	0.840	53.89	79.07	76.78	0.222	-
TargetM6A	79.45	77.88	78.67	0.573	0.847	53.68	78.02	75.81	0.210	0.708

[*]Results excerpted from [27].

This article has been accepted for publication in a future issue of this journal, but has not been fully edited. Content may change prior to final publication. Citation information: DOI 10.1109/TNB.2016.2599115, IEEE Transactions on NanoBioscience

motif near sequence terminals or a query RNA sequence shorter than 51-nt), the previously proposed "mirror image" technique [26] is used to fill in the missing nucleotides.

IV. Conclusions

In this study, we established a computational predictor for targeting the N^6-methyladenosine sites in RNA sequences. Inspired by the successful applications of the position-specific amino acid propensity features in proteomics, we introduced the new PSNP and PSDP features to encode RNA sequences. Based on the newly developed feature, we implemented an m^6A site predictor called TargetM6A. We compared the proposed TargetM6A method with the most recently released m^6A site predictors by performing stringent jackknife tests and independent validation tests on the benchmark datasets. The experimental results show that our TargetM6A method achieved high prediction performance and outperformed the existing predictors. A web-server has been placed online at http://csbio.njust.edu.cn/bioinf/TargetM6A to enhance the applicability of the proposed method. The findings of this study enrich our understanding of sequence-based m^6A sites and can potentially be applied to other nucleotide sequence-related prediction problems.

References

[1] K. C. Chou, "Impacts of bioinformatics to medicinal chemistry," Med Chem, vol. 11, pp. 218-34, 2015.

[2] C. Yi and T. Pan, "Cellular dynamics of RNA modification," Acc Chem Res, vol. 44, pp. 1380-8, Dec 20 2011.

[3] C. He, "Grand challenge commentary: RNA epigenetics?," Nat Chem Biol, vol. 6, pp. 863-5, Dec 2010.

[4] W. A. Cantara, P. F. Crain, J. Rozenski, J. A. McCloskey, K. A. Harris, X. Zhang, et al., "The RNA Modification Database, RNAMDB: 2011 update," Nucleic Acids Res, vol. 39, pp. D195-201, Jan 2011.

[5] A. Czerwoniec, S. Dunin-Horkawicz, E. Purta, K. H. Kaminska, J. M. Kasprzak, J. M. Bujnicki, et al., "MODOMICS: a database of RNA modification pathways. 2008 update," Nucleic Acids Res, vol. 37, pp. D118-21, Jan 2009.

[6] Y. Fu, D. Dominissini, G. Rechavi, and C. He, "Gene expression regulation mediated through reversible m(6)A RNA methylation," Nat Rev Genet, vol. 15, pp. 293-306, May 2014.

[7] G. Jia, Y. Fu, and C. He, "Reversible RNA adenosine methylation in biological regulation," Trends in Genetics, vol. 29, pp. 108-115, 2013.

[8] X. Wang, Z. Lu, A. Gomez, G. C. Hon, Y. Yue, D. Han, et al., "N6-methyladenosine-dependent regulation of messenger RNA stability," Nature, vol. 505, pp. 117-20, Jan 2 2014.

[9] K. D. Meyer and S. R. Jaffrey, "The dynamic epitranscriptome: N6-methyladenosine and gene expression control," Nat Rev Mol Cell Biol, vol. 15, pp. 313-26, May 2014.

[10] J. Liu, Y. Yue, D. Han, X. Wang, Y. Fu, L. Zhang, et al., "A METTL3-METTL14 complex mediates mammalian nuclear RNA N6-adenosine methylation," Nat Chem Biol, vol. 10, pp. 93-5, Feb 2014.

[11] X. L. Ping, B. F. Sun, L. Wang, W. Xiao, X. Yang, W. J. Wang, et al., "Mammalian WTAP is a regulatory subunit of the RNA N6-methyladenosine methyltransferase," Cell Res, vol. 24, pp. 177-89, Feb 2014.

[12] G. Jia, Y. Fu, X. Zhao, Q. Dai, G. Zheng, Y. Yang, et al., "N6-methyladenosine in nuclear RNA is a major substrate of the obesity-associated FTO," Nat Chem Biol, vol. 7, pp. 885-7, Dec 2011.

[13] G. Zheng, J. A. Dahl, Y. Niu, P. Fedorcsak, C. M. Huang, C. J. Li, et al., "ALKBH5 is a mammalian RNA demethylase that impacts RNA metabolism and mouse fertility," Mol Cell, vol. 49, pp. 18-29, Jan 10 2013.

[14] R. Desrosiers, K. Friderici, and F. Rottman, "Identification of methylated nucleosides in messenger RNA from Novikoff hepatoma cells," Proc Natl Acad Sci U S A, vol. 71, pp. 3971-5, Oct 1974.

[15] X. Deng, K. Chen, G. Z. Luo, X. Weng, Q. Ji, T. Zhou, et al., "Widespread occurrence of N6-methyladenosine in bacterial mRNA," Nucleic Acids Res, vol. 43, pp. 6557-67, Jul 27 2015.

[16] N. Liu, Q. Dai, G. Zheng, C. He, M. Parisien, and T. Pan, "N(6)-methyladenosine-dependent RNA structural switches regulate RNA-protein interactions," Nature, vol. 518, pp. 560-4, Feb 26 2015.

[17] C. R. Alarcon, H. Lee, H. Goodarzi, N. Halberg, and S. F. Tavazoie, "N6-methyladenosine marks primary microRNAs for processing," Nature, vol. 519, pp. 482-5, Mar 26 2015.

[18] C. Xu, X. Wang, K. Liu, I. A. Roundtree, W. Tempel, Y. Li, et al., "Structural basis for selective binding of m6A RNA by the YTHDC1 YTH domain," Nat Chem Biol, vol. 10, pp. 927-9, Nov 2014.

[19] D. Theler, C. Dominguez, M. Blatter, J. Boudet, and F. H. Allain, "Solution structure of the YTH domain in complex with N6-methyladenosine RNA: a reader of methylated RNA," Nucleic Acids Res, vol. 42, pp. 13911-9, Dec 16 2014.

[20] S. Kellner, J. Burhenne, and M. Helm, "Detection of RNA modifications," RNA Biol, vol. 7, pp. 237-47, Mar-Apr 2010.

[21] D. Dominissini, S. Moshitch-Moshkovitz, M. Salmon-Divon, N. Amariglio, and G. Rechavi, "Transcriptome-wide mapping of N6-methyladenosine by m6A-seq based on immunocapturing and massively parallel sequencing," Nature Protocols, vol. 8, pp. 176-189, 2013.

[22] K. D. Meyer, Y. Saletore, P. Zumbo, O. Elemento, C. E. Mason, and S. R. Jaffrey, "Comprehensive analysis of mRNA methylation reveals enrichment in 3' UTRs and near stop codons," Cell, vol. 149, pp. 1635-46, Jun 22 2012.

[23] Y. Li, X. Wang, C. Li, S. Hu, J. Yu, and S. Song, "Transcriptome-wide N(6)-methyladenosine profiling of rice callus and leaf reveals the presence of tissue-specific competitors involved in selective mRNA modification," RNA Biol, vol. 11, pp. 1180-8, 2014.

[24] S. Schwartz, Sudeep D. Agarwala, Maxwell R. Mumbach, M. Jovanovic, P. Mertins, A. Shishkin, et al., "High-Resolution Mapping Reveals a Conserved, Widespread, Dynamic mRNA Methylation Program in Yeast Meiosis," Cell, vol. 155, pp. 1409-1421, 2013.

[25] D. Dominissini, S. Moshitch-Moshkovitz, S. Schwartz, M. Salmon-Divon, L. Ungar, S. Osenberg, et al., "Topology of the human and mouse m6A RNA methylomes revealed by m6A-seq," Nature, vol. 485, pp. 201-6, May 10 2012.

[26] W. Chen, P. Feng, H. Ding, H. Lin, and K.-C. Chou, "iRNA-Methyl: Identifying N6-methyladenosine sites using pseudo nucleotide composition," Analytical Biochemistry, vol. 490, pp. 26-33, 2015.

[27] W. Chen, H. Tran, Z. Liang, H. Lin, and L. Zhang, "Identification and analysis of the N(6)-methyladenosine in the Saccharomyces cerevisiae transcriptome," Sci Rep, vol. 5, p. 13859, 2015.

[28] Z. Liu, X. Xiao, D. J. Yu, J. Jia, W. R. Qiu, and K. C. Chou, "pRNAm-PC: Predicting N-methyladenosine sites in RNA sequences via physical-chemical properties," Anal Biochem, vol. 497, pp. 60-67, Dec 31 2015.

[29] Y. Liu, W. Gu, W. Zhang, and J. Wang, "Predict and Analyze Protein Glycation Sites with the mRMR and IFS Methods," Biomed Res Int, vol. 2015, p. 561547, 2015.

[30] J. Wang, D. Zhang, and J. Li, "PREAL: prediction of allergenic protein by maximum Relevance Minimum Redundancy (mRMR) feature selection," BMC Syst Biol, vol. 7 Suppl 5, p. S9, 2013.

[31] C. Zou, J. Gong, and H. Li, "An improved sequence based prediction protocol for DNA-binding proteins using SVM and comprehensive feature analysis," BMC bioinformatics, vol. 14, p. 90, 2013.

[32] H. Liu and R. Setiono, "Incremental Feature Selection," Applied Intelligence, vol. volume 9, pp. 217-230(14), 1998.

[33] C. Cortes and V. Vapnik, "Support-vector networks," Machine Learning, vol. 20, pp. 273-297, 1995/09/01 1995.

[34] J. Brayet, F. Zehraoui, L. Jeanson-Leh, D. Israeli, and F. Tahi, "Towards a piRNA prediction using multiple kernel fusion and support vector machine," Bioinformatics, vol. 30, pp. i364-70, Sep 1 2014.

[35] E. K. Mohamed Hashim and R. Abdullah, "Rare k-mer DNA: Identification of sequence motifs and prediction of CpG island and promoter," J Theor Biol, vol. 387, pp. 88-100, Dec 21 2015.

[36] H. Vinje, K. H. Liland, T. Almoy, and L. Snipen, "Comparing K-mer based methods for improved classification of 16S sequences," BMC bioinformatics, vol. 16, p. 205, 2015.

[37] S. H. Guo, E. Z. Deng, L. Q. Xu, H. Ding, H. Lin, W. Chen, et al., "iNuc-PseKNC: a sequence-based predictor for predicting nucleosome positioning in genomes with pseudo k-tuple nucleotide composition," Bioinformatics, vol. 30, pp. 1522-1529, 2014.

[38] H. Lin, E. Z. Deng, H. Ding, W. Chen, and K. C. Chou, "iPro54-PseKNC: a sequence-based predictor for identifying sigma-54 promoters in prokaryote with pseudo k-tuple nucleotide composition," Nucleic Acids Research, vol. 42, pp. 12961-12972, 2014.
[39] K. C. Chou, "A vectorized sequence-coupling model for predicting HIV protease cleavage sites in proteins," J Biol Chem, vol. 268, pp. 16938-48, Aug 15 1993.
[40] M. C. Frith, U. Hansen, and Z. Weng, "Detection of cis-element clusters in higher eukaryotic DNA," Bioinformatics, vol. 17, pp. 878-89, Oct 2001.
[41] Y. R. Tang, Y. Z. Chen, C. A. Canchaya, and Z. Zhang, "GANNPhos: a new phosphorylation site predictor based on a genetic algorithm integrated neural network," Protein Eng Des Sel, vol. 20, pp. 405-12, Aug 2007.
[42] A. M. Thangakani, S. Kumar, R. Nagarajan, D. Velmurugan, and M. M. Gromiha, "GAP: towards almost 100 percent prediction for beta-strand-mediated aggregating peptides with distinct morphologies," Bioinformatics, vol. 30, pp. 1983-90, Jul 15 2014.
[43] Y. Xu, Y. X. Ding, J. Ding, L. Y. Wu, and N. Y. Deng, "Phogly-PseAAC: Prediction of lysine phosphoglycerylation in proteins incorporating with position-specific propensity," J Theor Biol, vol. 379, pp. 10-5, Aug 21 2015.
[44] A. Golugula, G. Lee, and A. Madabhushi, "Evaluating feature selection strategies for high dimensional, small sample size datasets," Conf Proc IEEE Eng Med Biol Soc, vol. 2011, pp. 949-52, 2011.
[45] Y. Mao, X. Zhou, D. Pi, Y. Sun, and S. T. Wong, "Multiclass cancer classification by using fuzzy support vector machine and binary decision tree with gene selection," J Biomed Biotechnol, vol. 2005, pp. 160-71, Jun 30 2005.
[46] V. N. Vapnik, "An overview of statistical learning theory," IEEE Trans Neural Netw, vol. 10, pp. 988-99, 1999.
[47] C. C. Chang and C. J. Lin, "LIBSVM: a Library for Support Vector Machines," Acm Transactions on Intelligent Systems & Technology, vol. 2, pp. 389-396, 2006.
[48] D. J. Yu, J. Hu, J. Yang, H. B. Shen, J. Tang, and J. Y. Yang, "Designing template-free predictor for targeting protein-ligand binding sites with classifier ensemble and spatial clustering," IEEE/ACM Trans Comput Biol Bioinform, vol. 10, pp. 994-1008, Jul-Aug 2013.
[49] D. J. Yu, J. Hu, H. Yan, X. B. Yang, J. Y. Yang, and H. B. Shen, "Enhancing protein-vitamin binding residues prediction by multiple heterogeneous subspace SVMs ensemble," BMC bioinformatics, vol. 15, p. 297, 2014.
[50] K. C. Chou and C. T. Zhang, "Prediction of protein structural classes," Crit Rev Biochem Mol Biol, vol. 30, pp. 275-349, 1995.
[51] K.-C. Chou, "Some remarks on protein attribute prediction and pseudo amino acid composition," J Theor Biol, vol. 273, pp. 236-247, 2011.
[52] K. C. Chou, "Using subsite coupling to predict signal peptides," Protein Eng, vol. 14, pp. 75-9, Feb 2001.
[53] W. Chen, H. Ding, P. Feng, H. Lin, and K. C. Chou, "iACP: a sequence-based tool for identifying anticancer peptides," Oncotarget, vol. 7, pp. 16895-909, Mar 29 2016.
[54] K. C. Chou, Z. C. Wu, and X. Xiao, "iLoc-Hum: using the accumulation-label scale to predict subcellular locations of human proteins with both single and multiple sites," Mol Biosyst, vol. 8, pp. 629-41, Feb 2012.
[55] X. Xiao, P. Wang, W. Z. Lin, J. H. Jia, and K. C. Chou, "iAMP-2L: a two-level multi-label classifier for identifying antimicrobial peptides and their functional types," Anal Biochem, vol. 436, pp. 168-77, May 15 2013.
[56] K. C. Chou, "Some remarks on predicting multi-label attributes in molecular biosystems," Mol Biosyst, vol. 9, pp. 1092-100, Jun 2013.
[57] D. J. Yu, J. Hu, Y. Huang, H. B. Shen, Y. Qi, Z. M. Tang, et al., "TargetATPsite: A template-free method for ATP-binding sites prediction with residue evolution image sparse representation and classifier ensemble," Journal of Computational Chemistry, vol. 34, pp. 974-985, 2013.
[58] T. Fawcett, "An introduction to ROC analysis," Pattern Recognition Letters, vol. 27, pp. 861-874, 2006.
[59] L. Breiman, "Random forests," Machine learning, vol. 45, pp. 5-32, 2001.
[60] T. M. Cover and P. E. Hart, "Nearest neighbor pattern classification," IEEE Transactions on Information Theory, vol. 13, pp. 21-27, 1967.
[61] S. F. Altschul, W. Gish, W. Miller, E. W. Myers, and D. J. Lipman, "Basic local alignment search tool," J Mol Biol, vol. 215, pp. 403-10, Oct 5 1990.
[62] J. O. Williams, "Narrow-band analyzer," Ph.D. dissertation, Dept. Elect. Eng., Harvard Univ., Cambridge, MA, 1993

Guang-Qing Li received his B.S. degree in computer science and technology from Nanjing University of Science and Technology in 2014. Currently, he is working towards the M.S. degree in the School of Computer Science and Engineering, Nanjing University of Science and Technology, China. His research interests include bioinformatics, data mining, and pattern recognition.

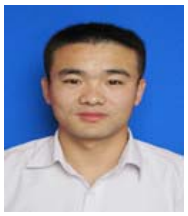

Zi Liu received his M.S. degree in computer science and technology from Jingdezhen Ceramic Institute China in 2015. Currently, he is working towards the Ph.D. degree in the School of Computer Science and Engineering, Nanjing University of Science and Technology, China. His research interests include bioinformatics, biomedical image processing, and pattern recognition.

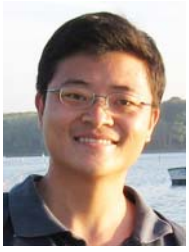

Hong-Bin Shen received his Ph.D. degree from Shanghai Jiaotong University China in 2007. He was a postdoctoral research fellow of Harvard Medical School from 2007 to 2008. Currently, he is a professor of Institute of Image Processing and Pattern Recognition, Shanghai Jiaotong University. His research interests include data mining, pattern recognition, and bioinformatics. Dr. Shen has published more than 60 papers and constructed 20 bioinformatics severs in these areas and he serves the editorial members of several international journals.

Dong-Jun Yu received the B.S. degree in computer science and the MS degree in artificial intelligence from Jiangsu University of Science and Technology in 1997 and 2000, respectively, and the Ph.D. degree in pattern analysis and machine intelligence from Nanjing University of Science and Technology in 2003. In 2008, he acted as an academic visitor at University of York in UK. He is currently a professor in the School of Computer Science and Engineering of Nanjing University of Science and Technology. His current interests include bioinformatics, pattern recognition, and data mining. He is a member of IEEE and CCF.